Speed up of Wave-Driven Unmanned Surface Vehicle Using Passively Transformable Two-segment Foils

Lyucheng Xie, Hongzheng Cui and Tin Lun Lam, *Senior Member, IEEE*

***Abstract*— For wave-driven unmanned surface vehicles (WUSVs), utilizing oscillating foils is the most straightforward and common wave energy conversion mechanism. Improving the thrust of the oscillating foil to increase its speed can help WUSVs improve their maneuverability and shorten the completion of ocean missions. This paper proposes a novel transformable two-segment foil, improving the wave energy-converting efficiency to provide more average thrust in every wave cycle. We estimate their working effectiveness numerically with a simple model to verify that the design enhances foils' thrust force. The thrust enhancement was further confirmed by computational fluid dynamic (CFD) simulations, and we estimated the suitable values of parameters of the foils in several different common sea conditions in coastal waters by CFD simulations. We design and make two wave gliders with traditional and transformable two-segment foils and finish the speed enhancement experiments. The speed enhancement is verified, and transformable two-segment foils can increase the speed of WUSVs by 10% in similar sea conditions in experiments.**

I. INTRODUCTION

In recent years, unmanned control and energy self-sufficiency have been widely applied and developed in detecting and monitoring the ocean [1]–[4]. Compared with the limited self-carrying energy, such as gasoline and batteries, marine renewable energy has an absolute advantage in terms of endurance. There are some common unmanned surface vehicles shown in Table. I. We find that wave-driven vehicles tend to have longer voyage distances but lower sailing speeds.

The wave glider, a wave-driven unmanned surface vehicle (WUSV) equipped with solar panels, plays an increasingly important role in fields like ocean data collection [1], [5], due to wave energy stability. The WUSV comprises a surface float, and a underwater glider with oscillating foils, connected by a cable [3], [6].

This work was supported by the opening project of Guangdong Provincial Key Lab of Robotics and Intelligent System and the funding AC01202101103 from the Shenzhen Institute of Artificial Intelligence and Robotics for Society.(*Corresponding author: Tin Lum Lam.*)

Lyucheng Xie and Tin Lun Lam are with the School of Science and Engineering, The Chinese University of Hong Kong, Shenzhen, Guangdong;Shenzhen Institute of Artificial Intelligence and Robotics for Society (AIRS), The Chinese University of Hong Kong, Shenzhen, Guangdong, 518172, P.R.China (email:873533907@qq.com; tllam@cuhk.edu.cn).

Hongzheng Cui is student in Engineering Faculty in Monash University, Melbourne, Australia (email:2766073705@qq.com).

TABLE I
SURFACE VEHICLE PERFORMANCE [7]

Vehicle	Propulsion	Average Speed(knt)	Voyage (NM)
AutoNaut [8]	Wave Foil	4	6500
C-Enduro [9]	Electric Propeller	3.5	7500
Saildrone [10]	Rigid Sail	4	2250
Wave Glider [11]	Wave Foil	1.8	9000

As a wave-driven vehicle, its propulsion is wave energy [12]. Wave foil is a common wave energy conversion device. When the vehicle rises and falls with the waves, it will generate a vertical relative flow to the foils, resulting in the foils pitching down and up, as shown in Fig. 1, by which the foils convert the wave energy into forwarding thrust force, which realizes the conversion from wave energy to the kinetic energy of wave glider in this hydrodynamic process. The movement of foils in every wave cycle is composed of 5 steps: (1) initially at the up boundary where the angle between the foil and the horizontal is the upper limit angle (The sizes of the limit angles are controlled by our limit device.) and start to swing down at t_0; (2) swing and reach the down boundary at time t_1; (3) hold at this position until start to swing up at time t_2; (4) swing and reach the up boundary at time t_3; (5) hold at this position until swing down again at time t_4.

In the study of increasing WUSV's speed, improving energy conversion efficiency are primary, especially for the design of oscillating foils [13]. Some previous studies focused on facilitating the utilization of wave energy. The critical pitching amplitude can improve the propulsive performance of semi-active flapping foil [13]. The motion performance can be optimized for oscillating foils in these four parameters: the geometric parameter, performance parameter, kinematic parameter, and environmental parameter [14]. Some researchers have experimented with geometric parameters to advance the achievement in complex ocean environments. The shape of flapping foils is a crucial factor.

In the spectral difference (SD) numerical investigation of NACA type foils' propulsion conduct, thin foils act advantageously [15]. Moreover, researchers found they could raise the thrust force of wave gilder by using lower aspect-ratio foils [16]. Additionally, inspired by the bionic, investigators assume a foil as an unalterable line by neglecting the foil's thickness and shape [17].

A specific range of degrees is also found to exert positive effects on symmetry preservation for flexible wings, otherwise giving rise to symmetry-breaking of flexible wings in

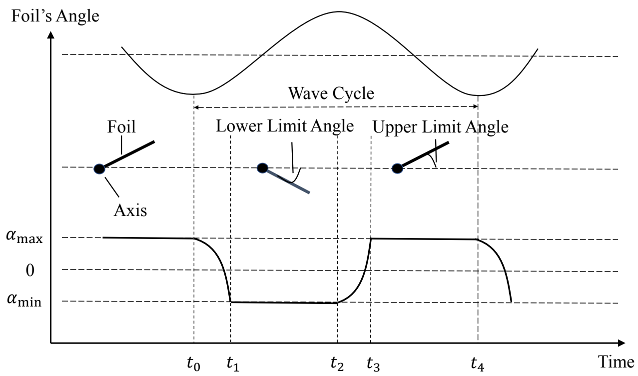

Fig. 1. The view of the movement of a passive-motion foil in one wave cycle and the change of the angle between foil and horizontal.

incompressible and laminar flows. [18].

Most previous studies focused on parameters of inflexible foil. In this paper, we design a novel transformable two-segment foil for the first time, and the submerged motion state of this new wave glider under the water is shown in Fig. 2. We choose several common sea conditions in coastal waters to simulate to confirm that transformable two-segment foil can increase the speed of WUSVs. Moreover, we finished speed enhancement experiments, finding that the wave glider's speed increased by 10%.

This paper is composed of six sections. Section II will introduce the transformable two-segment foils and describe the trajectories of that at certain times. Section III is a numerical estimation of thrust increment of transformable two-segment foil. There will be the corresponding CFD simulations of impulse in Section IV and the actual experiment procedures in Section V. The conclusion of transformable two-segment foils performance and future work will be presented in Section VI.

II. DESIGN OF TRANSFORMABLE TWO-SEGMENT FOIL

We have proposed one kind of asymmetric foil that can improve the propeller's thrust force provided to the WUSVs [19], [20]. The foil can not be transformed, and it will cause a thrust loss at the upper limit angle. A transformable foil can be transformed to fit both the upper and lower limit angles and can reach a better thrust enhancement effect.

We design one kind of novel transformable two-segment foil formed by combining two segment foils, a stopper and a transmission shaft (Axis 2) between two segment foils, which can be deformed to fit both the upper and lower limit angles. The schematic diagram of the transformable two-segment foil trajectories is shown in Fig. 2. Because of WUSV's heaving and pitching motions with the wave, there is a vertical relative water flow to the foils, which leads to the flapping around a transmission shaft (Axis 1) fixed to the hull with locks.

The first angular limitation to achieve the first limiting angle is α. In addition, the second limitation to accomplish the second one is β, which sets the boundaries of the second segment foil. The stopper is designed to prevent the motion failure caused by the relative rotation of two foils beyond a specific position range.

This schematic diagram of the foils movement cycle consists of six steps in every wave period, as shown in Fig. 3:

Step 1: Wave glider is falling. The foils stay at upper boundaries. The angle α between the first segment foil and the horizontal is the first upper limit angle, and the angle β between the second one and the horizontal is the second upper limit angle.

Step 2: Wave glider begins to rise. Both segments of foil swing down with a fixed angle between them because of the stopper.

Step 3: Wave glider is rising. The second segment foil arrives at the second lower limitation device, and relative rotation occurs between two segments until the first segment foil arrives at the first lower limitation device. The angle between two segment foils reverses in a tiny period because of inertia. The first segment foil touches the upper end of the stopper when it arrives at the lower angular limitation.

Step 4: Wave glider is rising. The foils initially stay at the lower boundaries.

Step 5: Wave glider begins to fall. Both segments of foil swing up with a fixed angle between them because of the stopper.

Step 6: Wave glider is falling. The second segment foil arrives at the second upper limitation device. After relative rotation between two segment foils, the first segment foil touches the lower end of the stopper when it arrives at the upper angular limitation. The state of the transformable two-segment foil is the same.

The transformable two-segment foil stays at the boundaries where the maximum thrust is in most time intervals in one wave cycle.

III. NUMERICAL ESTIMATE OF AVERAGE THRUST INCREMENT

In this section, we complete numerical estimation to demonstrate that our transformable two-segment foil can receive more average thrust than a traditional foil in the same wave cycle. In order to verify that transformable two-segment foils could provide more average thrust, we estimate the impulse in one wave cycle, which is proportional to the average thrust.

A. Water Velocity on Surface of the Foil

To simplify the calculation model, we assume that the water is an ideal fluid and ignore viscous damping. We can estimate water velocity on the surface of the foil by using the panel method [21].

We choose k control points with proper spacing on the foil's surface and make sections of the object through control points. The foil's surface can be replaced by several panels. We put point sources and vortexes on the panels, reflecting the water and foil interaction. Moreover, we assume that the

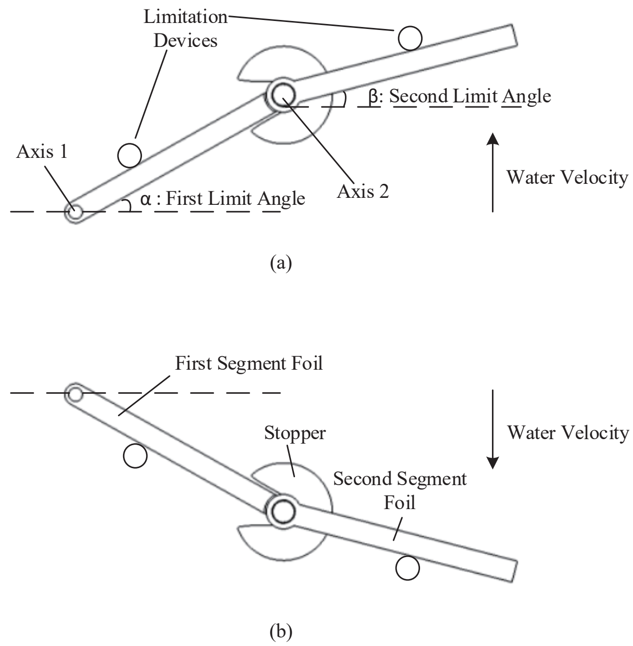

Fig. 2. (a) Upper limit position of the transformable two-segment foils and the introduction of components. (b) Lower limit position of the transformable two-segment foils and the introduction of components.

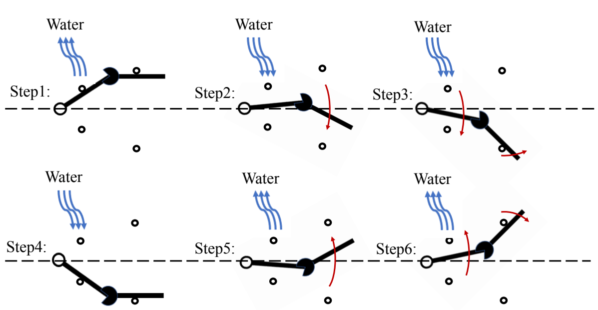

Fig. 3. Schematic diagram of transformable two-segment foil's movement cycle.

intensity of the source and vortex distribution on the same panel is consistent. The point source intensity of panel j is q_j and the point vortex intensity of panel j is γ_j.

Φ_j, the velocity potential generated by sources on panel j, and Ψ_j, velocity potential generated by vortexes on panel j, can be expressed as Eq. 1.

$$\begin{cases} \Phi_j = \dfrac{q_j}{2\pi}\displaystyle\int_{S_j} \ln\sqrt{(x-x_j)^2+(y-y_j)^2}\, dS_j \\ \Psi_j = \dfrac{\gamma_j}{2\pi}\displaystyle\int_{S_j} \arctan\dfrac{y-y_j}{x-x_j}\, dS_j \end{cases} \tag{1}$$

where S_j is the area of panel j.

For any panel i, the water Velocity in the normal direction from both point source velocity potential and point vortex velocity potential on the surface is zero. Because of that, we can build the Eq. 2:

$$\begin{cases} v_\infty \dfrac{\partial x}{\partial n_i} + \displaystyle\sum_{j=1}^{k} \dfrac{\partial \Phi_j}{\partial n_i} = 0,\ i = 1,...,k \\ \displaystyle\sum_{j=1}^{k} \dfrac{\partial \Psi_j}{\partial n_i} = 0,\ i = 1,...,k \end{cases} \tag{2}$$

where v_∞ is the inflow velocity.

The Eq. 2 contains $2k$ equations and $2k$ unknowns(q_j and γ_j). In order to prevent solving for trivial solutions, we need to add the following equations. v_{Si} is the water velocity on the panel's surface i. q_i.

$$v_{Si} = v_\infty \frac{\partial y}{\partial S_i} + \sum_{j=1}^{k} \frac{\partial \Phi_j}{\partial S_i} + \sum_{j=1}^{k} \frac{\partial \Psi_j}{\partial S_i} \tag{3}$$

Accoding to Kutta-Joukowski condition,

$$v_{S1} = v_{Sk} \tag{4}$$

q_j, γ_i, and v_{Si} can be solved from Eqs. 1 to 4.

B. Thrust Force

According the v_{Si} solved from Eqs. 1 to 4, pressure distribution p_i can be calculated using Bernoulli's principle. F_{px} can be expressed as:

$$F_{px}(\alpha, \beta) = \sum_{i=1}^{k} \int_{S_i} p_i \cos\theta_i \, dS_i \tag{5}$$

where θ_i is the angle between the direction of S_i and the horizontal. It can be solved numerically by substituting the assumed parameters.

C. Motion Model of Transformable Two-segment Foil

Here we assume that the horizontal speed of foil is zero because the horizontal speed (sailing speed) is related to the overall motion of the WUSV, and the value of this speed can not be obtained only by numerical calculation. The horizontal inflow velocity is zero, and the vertical inflow velocity can be expressed as:

$$v_\infty(t) = A\cos(\omega t) \tag{6}$$

where A is amplitude and ω is angular velocity.

During rotation, the foil can be treated as a rigid body most of the time. The rotational inertia can be expressed as:

$$I = \int r^2 \rho(s) w(s)\, ds \tag{7}$$

where ρ denotes the foil's density, r denotes the distance from the origin.

The moment of force can be expressed as:

$$M = -\vec{r} \times \vec{n} \int_{S_i} p_i \, dS_i \tag{8}$$

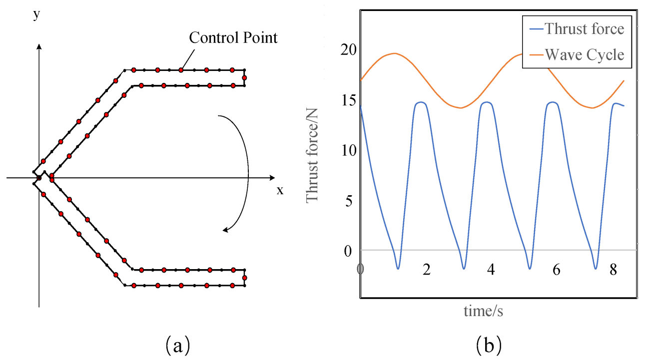

Fig. 4. (a) Control Points Of Transformable two-segment Foil. (b) Thrust force of transformable two-segment foil during the wave cycle. $A = 0.3\ m$, $T = 2\ s$, width $w = 35\ cm$, thickness $D = 0.5\ cm$, length $L = 11\ cm$, first limit angle $\alpha = 40°$, second limit angle $\beta = 10°$.

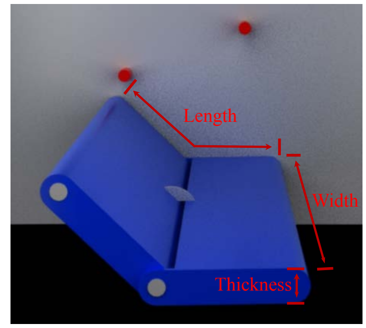

Fig. 5. Parameters of transformable two-segment foil

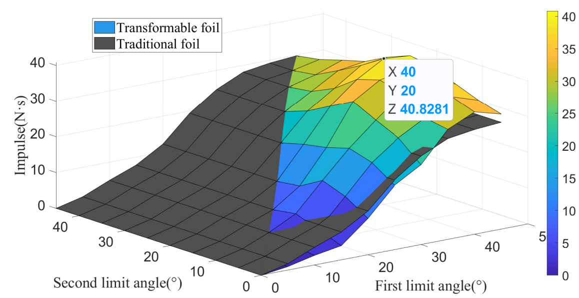

Fig. 6. Numerical calculation: the impulse of transformable two-segment foil in one wave cycle with different parameter pairs (first limit angle and second limit angle), WMO sea state code:2, Wave height= 0.6 m, $T = 4\ s$, width $w = 35\ cm$, thickness $D = 0.5\ cm$, length $L = 11\ cm$.

where $\vec{n}$ is normal vector of S_i

Divide the angle of oscillation equally into n angles and assume that the thrust force, the moment of force, and the angular acceleration are fixed values in one angle i. According to definitions of angular velocity and angular acceleration, we can get kinetic equations:

$$\begin{cases} \omega_{t_i} = \omega_{t_{i-1}} + \beta_{t_{i-1}}(t_i - t_{i-1}),\ i = 1, ..., n \\ \dfrac{2a}{n} = \dfrac{1}{2}(\omega_{t_i} + \omega_{t_{i-1}})(t_i - t_{i-1})\ i = 1, ..., n \\ \beta_{t_i} = \dfrac{M_i}{I}\ i = 0, ..., n-1 \\ \omega_{t_0} = 0 \end{cases} \tag{9}$$

where t_i is the time when foil swing into angle i, ω_{t_i} is the angular velocity of foil in angle i, β_{t_i} is the angular acceleration of foilin angle i and M_i is the moment of force of foil in angle i.

M_i, β_i, t_i and F_{pxt} can be solved from Eqs. 6 to 9.

D. Impulse in One Wave Cycle

When the foil reaches the boundary, we divide the rest of the cycle into m periods and assume that the thrust force is uniform in one period. The impulse received by foil in one cycle can be expressed as:

$$P = 2(\sum_{i=0}^{n-1} F_{pxt}(t_{i+1} - t_i) + \sum_{j=0}^{m-1} F_{px}(\alpha, \beta, j)\frac{\frac{\pi}{\omega} - t_{n-1}}{m}) \tag{10}$$

E. Numerical Calculation

To preliminarily verify that our transformable two-segment foil can receive more impulse from water than a traditional foil in one wave cycle, we divide the transformable two-segment foil and traditional foil into 11 equal parts by 11 control points on each side, shown in Fig. 4(a). Other parameters chosen for transformable two-segment foil: width $w = 35\ cm$, thickness $D = 0.5\ cm$, length $L = 11\ cm$, shown in Fig.5 . The traditional foil has the same length, width, and thickness; in the traditional foil, the first limit angle is equal to the second limit angle. The wave conditions we choose are closed to conditions in the sea area of Daya Bay where we perform our experiment: wave height $A = 0.3\ m$, wave period $T = 4\ s$.

The impulse received by traditional foil and transformable two-segment foil is shown in Fig. 6. The grey plane is data of the traditional foil whose first limit angle equals the second limit angle. We can find that $40°$ is a suitable first limit angle to make the foils produce the large impulse with the parameters we chose, and $20°$ is a suitable second limit angle to make the foils receive the large impulse with the parameters we chose. The impulse received by transformable two-segment foil is bigger than the traditional foil with the first and second limit angles we have chosen. The most increment of impulse can reach 31.4% ((40.83N·s/31.06N·s)-1) . The thrust of transformable two-segment foil with suitable first limit angle and suitable second limit angle we got during the wave cycle is shown in Fig. 4(b).

IV. IMPULSE SIMULATION

In Section III, there are many ideal assumptions in formula derivation: flow field is instantaneous steady-state flow; the system friction, gravity and material deformation are ignored; two-dimensional flow field are considered. These make the calculation results have a certain deviation.

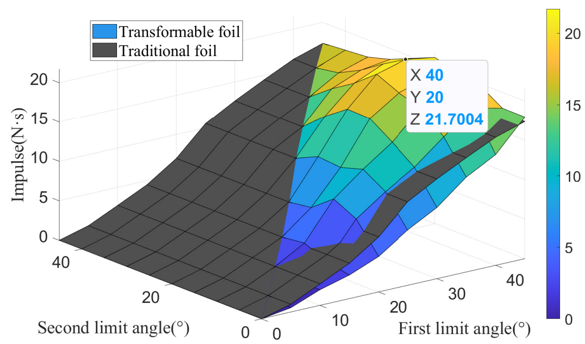

Fig. 7. Simulation result in sea condition a: the impulse of traditional foil and transformable two-segment foil in one wave cycle with different parameter pairs (first limit angle and second limit angle). WMO sea state code 2, wave height= $0.3\ m$, $T = 4.4\ s$, width $w = 35\ cm$, thickness $D = 0.5\ cm$, length $L = 11\ cm$.

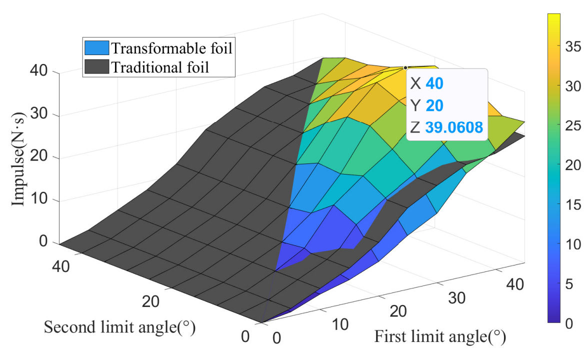

Fig. 8. Simulation result in sea condition b: the impulse of traditional foil and transformable two-segment foil in one wave cycle with different parameter pairs (first limit angle and second limit angle). WMO sea state code 2, wave height= $0.5\ m$, $T = 4.5\ s$, width $w = 35\ cm$, thickness $D = 0.5\ cm$, length $L = 11\ cm$.

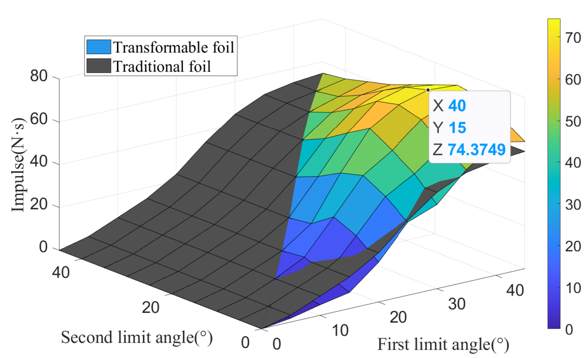

Fig. 9. Simulation result in sea condition c: the impulse of traditional foil and transformable two-segment foil in one wave cycle with different parameter pairs (first limit angle and second limit angle). WMO sea state code 2, wave height= $0.6\ m$, $T = 4\ s$, width $w = 35\ cm$, thickness $D = 0.5\ cm$, length $L = 11\ cm$.

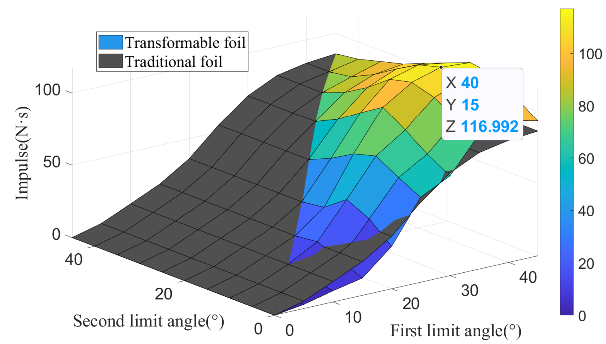

Fig. 10. Simulation result in sea condition d: the impulse of traditional foil and transformable two-segment foil in one wave cycle with different parameter pairs (first limit angle and second limit angle). WMO sea state code 3, wave height= $0.88\ m$, $T = 5.4\ s$, width $w = 35\ cm$, thickness $D = 0.5\ cm$, length $L = 11\ cm$.

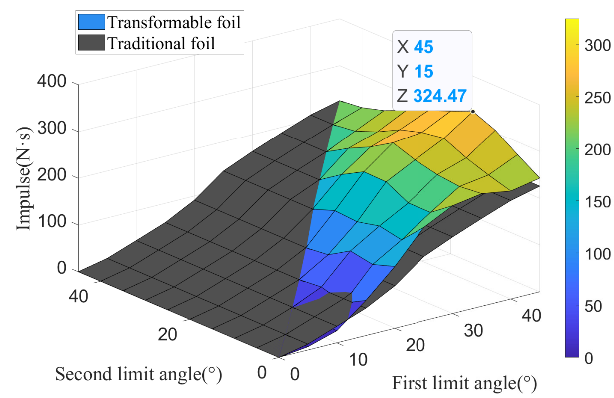

Fig. 11. Simulation result in sea condition e: the impulse of traditional foil and transformable two-segment foil in one wave cycle with different parameter pairs (first limit angle and second limit angle). WMO sea state code 4, wave height= $2\ m$, $T = 8.8\ s$, width $w = 35\ cm$, thickness $D = 0.5\ cm$, length $L = 11\ cm$.

In order to verify the impulse enhancement effect of our transformable two-segment foil in Section II, determine its two critical parameters in proper order: first limit angle, second limit angle, and then estimate the increment of WUSV's speed, we designed the corresponding CFD simulations using ANSYS 2022. Compared with numerical calculation, simulation has several advantages: flow field is unsteady; the system friction, gravity and material deformation are considered; three-dimensional flow field and fluid-solid coupling are considered.

We set the horizontal flow velocity received by foil to zero for the same reason as Section II. So we keep the forward speed consistent in all simulations, which can minimize its impact on the final simulation results. The material we chose is aluminium alloy.

To simulate the impulse, we divide one wave cycle evenly into 40 periods and assume that the trust foil received is uniform in one period. We choose the thrust simulated at the beginning of one period as the mean thrust of that period to get the impulse received by foil in one period. Summing up impulses, we can get an impulse in one wave cycle.

The impulse performance difference between the transformable two-segment foil we proposed with different parameters and the traditional foil is compared under the same wave conditions.

A. Impulse with different first limit angle and second limit angle

We choose several different common sea conditions to simulate. Sea conditions a to d are common sea conditions in coastal waters which are similar to sea conditions in our experiment site, and sea condition e is the most dominant sea state worldwide.

Through different limit angle simulations, the suitable limit angles of transformable two-segment foil to make the foils produce the large impulse in different wave conditions are shown in Fig. 7 to Fig. 11.

We can see that not all the transformable two-segment foil performs better than the traditional foil. In this simulation experiment, the largest impulse enhancement effect can reach 25.4% ((21.70N·s/17.36N·s)-1) in sea condition a, 31.8% ((39.06N·s/29.64N·s)-1) in sea condition b, 32.7% ((74.37N·s/56.04N·s)-1) in sea condition c, 35.7% ((116.99N·s/86.21N·s)-1) in sea condition d and 39.9% ((315.00N·s/225.2N·s)-1) in sea condition e.

B. Increment of speed

We use a simple model to simplify the numerical relationship between water resistance wave glider received and velocity of wave glider: the water resistance is proportionate to the square of velocity [22]:

$$R = Cv^2 \tag{11}$$

Where R is water resistance, C is a constant coefficient. The water resistance is approximately equal to the average thrust received by foil. Therefore, the square of velocity is proportionate to the impulse. The simulated increment of the speed of the wave glider is shown in Table II. It is worth mentioning that the impulse ratios in Table II are the ratios of the biggest impulses of transformable foil to the biggest impulses of traditional foil. The simulating results show that transformable two-segment foil can enhance the speed of WUSVs by between 12.0% and 16.5% in coastwise wave conditions, 20.3% in the most dominant sea state worldwide.

TABLE II
SIMULATION DATA

sea condition	a	b	c	d	e
sea state code	2	2	2	3	4
wave height/m	0.3	0.5	0.6	0.88	2.0
wave period/s	4.4	4.5	4	5.4	8.8
1st limit angle/°	40	40	40	40	45
2nd limit angle/°	20	20	15	15	10
impulse ratio	1.254	1.318	1.327	1.357	1.447
speed up/%	12.0	14.8	15.2	16.5	20.3

TABLE III
PARAMETERS OF THE WUSV

	Width	**Length**	**Thickness**
Backbone	1350 mm	150 mm	5 mm
Trad. Foil	350 mm	110 mm	5 mm
Tran. 1st foil	350 mm	55 mm	5 mm
Tran. 2nd foil	350 mm	55 mm	5 mm

TABLE IV
EXPERIMENTAL DATA

	Trad. Foil	**Tran. Foil**	**Ratio**
1st trial	0.1788 m/s	0.2004 m/s	1.121
2nd trial	0.1845 m/s	0.2056 m/s	1.097
3rd trial	0.1908 m/s	0.2064 m/s	1.082
Mean			1.100
Simulation			1.152
Asymmetric foil [20]			1.089

V. SPEED ENHANCEMENT EXPERIMENT

We designed and made two wave gliders: one is the experimental group with transformable two-segment foils, and the other is the control group with traditional foils. The speed test experiments were carried out in Daya Bay, Shenzhen.

A. Experimental preparation

Each WUSV is composed of the underwater glider and an inflatable stand-up paddleboard(float) with a cable, as shown in Fig. 12. Both wave gliders consist of a backbone, and six pairs of foils and foils can be installed on the axis by the assembly structure and sway around the axis, as shown in Fig. 13. We make the same body and equivalent size foils of the control group and the experimental group, which their width are 350mm, overall length are 110mm, and thickness are 5mm, as shown in Table III.

In addition, there are two position-limit mechanisms, as shown in Fig. 13. The first mechanism is an angle limitation: the arc holes where the connecting shaft swings in its designed angle range. The second mechanism is a position boundary, limiting the second segment foils' vertical positions. For wave gliders with traditional foils, we choose the first limit angle $\alpha = 45°$. For wave gliders with transformable two-segment foils, we choose first limit angle $\alpha = 45°$ and second limit angle $\beta = 15°$. The whole wave glider is 1350 mm long and 800 mm wide, including the 340 mm long foils, with the distance between every pair of neighbour foils being 150 mm. All detailed parameters are shown in Table III. The 1st and 2nd foil in the table means the first and second segment foil.

The wave glider drives the paddleboard forward by a cable. Some GPS positioning devices are also designed to fix every

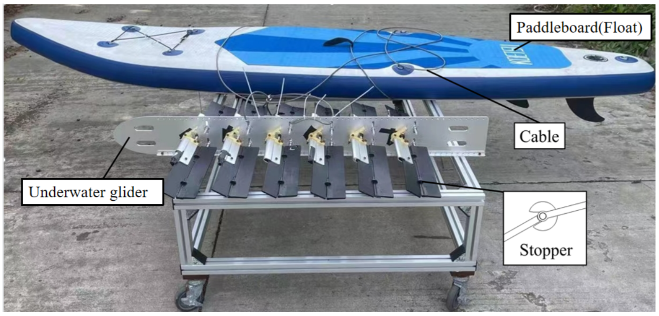

Fig. 12. The WUSV consists of several parts including the wave glider, connected to an inflatable stand-up paddleboard by the cable. The stoppers on the foils are to prevent the position limitation failure.

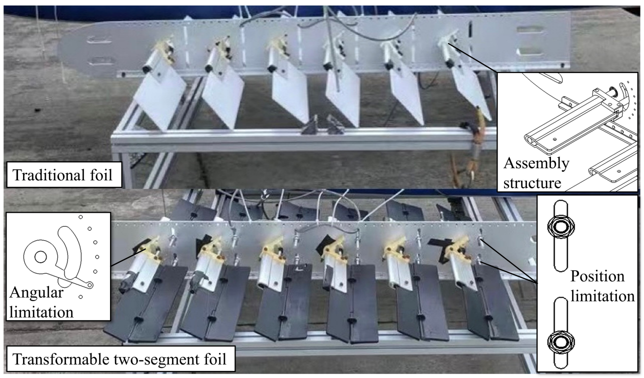

Fig. 13. The control group and the experimental group use traditional foils and transformable two-segment foils respectively. The installation of foils to the body uses the assembly structure. The angular limitation and position limitation are designed to limit foils movement range. The material of foils is Poly oxy methylene(POM) and the density is 1.42 g/cm^3.

paddleboard, which collects real-time statistics of each wave glider in experiments.

B. Speed enhancement experiment

The sea trials were carried out in the sea area of Daya Bay in Shenzhen, China. We got some pictures in the experiment, shown in Fig.14, 15.

We have 3 groups of experiment, experimental times and marine environments of them: (1)Time:$\sim$16:15 GMT+8, 27/08/2021; Wind: $\sim$2kt; Wave amplitude:0.2-0.3m (2) Time: $\sim$10:10 GMT+8, 28/08/2021; Wind: $\sim$3kt; Wave amplitude: 0.3-0.4m (3) Time: $\sim$15:20 GMT+8, 28/08/2021; Wind: $\sim$3kt; Wave amplitude: 0.3-0.4m. The marine navigation record is shown in Fig. 16, 17, 18.

The average speeds of wave gliders with transformable two-segment and traditional foils are shown in Table IV. The mean increment of the speed of the wave glider with transformable two-segment foils can reach 10%, which is larger than the wave glider with asymmetric foils.

In the most similar sea condition (sea condition c), the simulated increment of the speed of the wave glider can reach 15.2% in Section IV.

In comparison, the average speed increment in the simulation is lower than that in the simulation because some disturbances are not considered: in the real system, there will

Fig. 14. Surface float in experiment

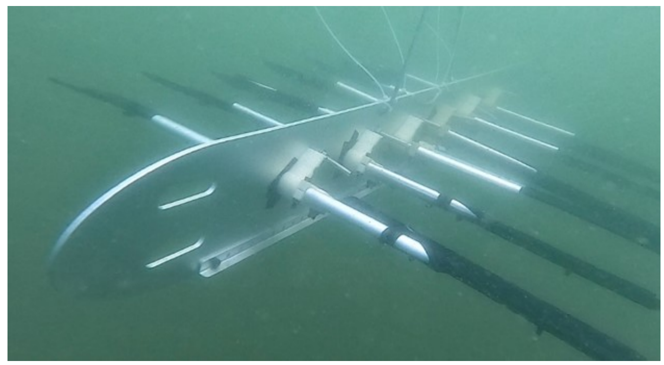

Fig. 15. Underwater glider in experiment

be coupling between the surface and underwater portions of the system through the connecting cable and the inertia (and added mass) of the components will an important impact on the response of the underwater foil system; wave radiation influence experimental results; the relative velocity between water and foil is not precisely vertical, etc. In addition, tolerance in manufacture gives rise to skewing from the ideal consequence.

Even so, the experiments verify that the transformable two-segment foils have superior performance to traditional ones.

VI. CONCLUSIONS AND FUTURE WORK

In this paper, one kind of novel transformable two-segment foil that fits both the upper and lower limit angles is proposed, which can improve the thrust of the propeller provided to the WUSVs. The numeric method, CFD simulations, and hydrodynamic experiments verify its thrust enhancement effect. The numerical simulating results show that transformable two-segment foil can enhance the speed of WUSVs by between 12.0% and 16.5% in coastwise wave conditions, 20.3% in the most dominant sea state worldwide. The experimental ones indicate the increment of 10% in the meanwhile.

There are several future works we can do: studying other parameters, including the length, width, thickness, materials of the foil, and the segment point's position; realizing the

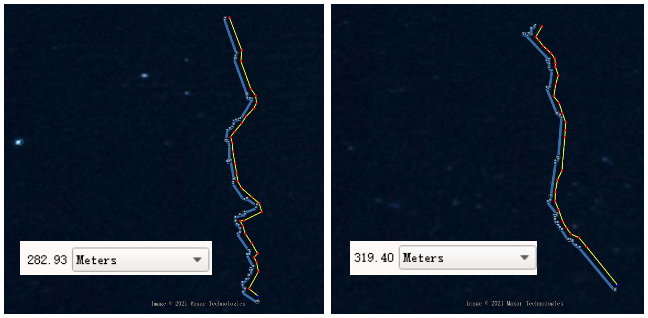

(a) (b)

Fig. 16. Team1: Wind: ∼2kt; Wave amplitude:0.2-0.3m (a)Sailing record of the wave glider with traditional foils; From 16:15:31 to 16:41:53 on GMT+8, 27/08/2021; The sailing distance is 282.91m. (b)Sailing record of the wave glider with transformable two-segment foils: 16:15:47 to 16:42:21 on GMT+8, 27/08/2021; The sailing distance is 319.40m.

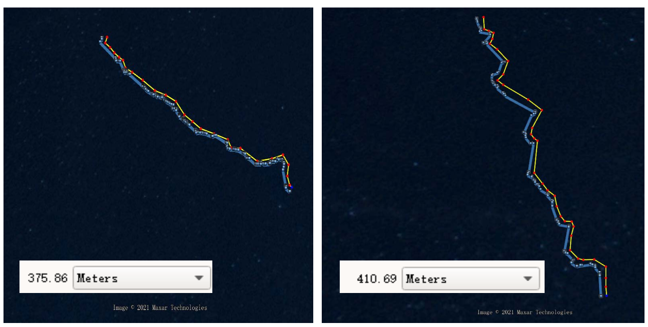

(a) (b)

Fig. 17. Team2: Wind: ∼3kt; Wave amplitude: 0.3-0.4m (a)Sailing record of the wave glider with traditional foils: From 10:13:10 to 10:47:07 on GMT+8, 28/08/2021; The sailing distance is 375.86m. (b)Sailing record of the wave glider with transformable two-segment foils: From 10:14:04 to 10:47:24 on GMT+8, 28/08/2021; The sailing distance is 410.69m.

dynamic simulation of foils considering the changes in the horizontal speed to get more accurate simulation results; conducting more far-sea experiments with enough resources to optimize our parameter selection; designing more transformable foil structures. For example, a transformable foil with more segments having more degrees of freedom may cope with more different conditions.

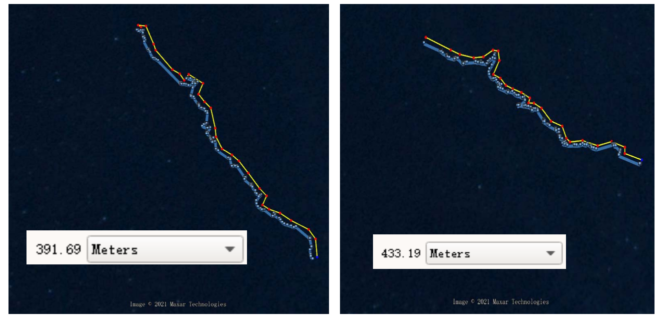

(a) (b)

Fig. 18. Team3: Wind: ∼3kt; Wave amplitude: 0.3-0.4m (a)Sailing record of the wave glider with traditional foils: From 15:23:01 to 15:57:13 on GMT+8, 28/08/2021; The sailing distance is 391.69m. (b)Sailing record of the wave glider with transformable two-segment foils: From 15:23:39 to 15:58:38 on GMT+8, 28/08/2021; The sailing distance is 433.19m.

REFERENCES

[1] R. Hine, S. Willcox, G. Hine, and T. Richardson, "The wave glider: A wave-powered autonomous marine vehicle," in *OCEANS 2009*, pp. 1–6, IEEE, 2009.
[2] P. Johnston and M. Poole, "Marine surveillance capabilities of the autonaut wave-propelled unmanned surface vessel (usv)," in *OCEANS 2017-Aberdeen*, pp. 1–46, IEEE, 2017.
[3] J. Manley and S. Willcox, "The wave glider: A persistent platform for ocean science," in *OCEANS'10 IEEE SYDNEY*, pp. 1–5, IEEE, 2010.
[4] B. Tian, J. Yu, A. Zhang, F. Zhang, Z. Chen, and K. Sun, "Dynamics an· alysis of wave-driven unmanned surface vehicle in longitudinal profile," in *OCEANS 2014-TAIPEI*, pp. 1–6, IEEE, 2014.
[5] B. Bingham, N. Kraus, B. Howe, L. Freitag, K. Ball, P. Koski, and E. Gallimore, "Passive and active acoustics using an autonomous wave glider," *Journal of field robotics*, vol. 29, no. 6, pp. 911–923, 2012.
[6] P. Wang, X. Tian, W. Lu, Z. Hu, and Y. Luo, "Dynamic modeling and simulations of the wave glider," *Applied Mathematical Modelling*, vol. 66, pp. 77–96, 2019.
[7] https://theliquidgrid.com/2017/07/11/autonomous-ocean-robots/.
[8] https://auvac.org/259-2-2/.
[9] https://www.unmannedsystemstechnology.com/wp-content/uploads/2013/12/C-Enduro-brochure.pdf/.
[10] https://www.saildrone.com/missions/.
[11] https://www.liquid-robotics.com/blog/.
[12] E. Filippas and K. Belibassakis, "Hydrodynamic analysis of flapping-foil thrusters operating beneath the free surface and in waves," *Engineering Analysis with Boundary Elements*, vol. 41, pp. 47–59, 2014.
[13] Z. Qi, B. Zou, H. Lu, J. Shi, G. Li, Y. Qin, and J. Zhai, "Numerical investigation of the semi-active flapping foil of the wave glider," *Journal of Marine Science and Engineering*, vol. 8, no. 1, p. 13, 2020.
[14] X. Wu, X. Zhang, X. Tian, X. Li, and W. Lu, "A review on fluid dynamics of flapping foils," *Ocean Engineering*, vol. 195, p. 106712, 2020.
[15] M. Yu, Z. Wang, and H. Hu, "High fidelity numerical simulation of airfoil thickness and kinematics effects on flapping airfoil propulsion," *Journal of Fluids and Structures*, vol. 42, pp. 166–186, 2013.
[16] J. Lee, Y.-J. Park, K.-J. Cho, D. Kim, and H.-Y. Kim, "Hydrodynamic advantages of a low aspect-ratio flapping foil," *Journal of Fluids and Structures*, vol. 71, pp. 70–77, 2017.
[17] X. Zhu, G. He, and X. Zhang, "Numerical study on hydrodynamic effect of flexibility in a self-propelled plunging foil," *Computers & Fluids*, vol. 97, pp. 1–20, 2014.
[18] G. K. Politis and V. Tsarsitalidis, "Simulating biomimetic (flapping foil) flows for comprehension, reverse engineering and design," in *First International Symposium on Marine Propulsors*, 2009.
[19] Y. Gao, L. Xie, and T. L. Lam, "Thrust enhancement of wave-driven unmanned surface vehicle by using asymmetric foil," in *2021 IEEE International Conference on Robotics and Automation (ICRA)*, pp. 758–764, IEEE, 2021.
[20] Y. Gao, L. Xie, and T. L. Lam, "A novel and more efficient oscillating foil for wave-driven unmanned surface vehicles," *Frontiers in Robotics and AI*, vol. 9, 2022.
[21] J. D. Anderson and J. Wendt, *Computational fluid dynamics*, vol. 206. Springer, 1995.
[22] X. Li, "Dynamic model and simulation study based on the wave glider," *China Ship Research and Development Academy: Beijing, China*, 2014.